Molecular composites formed by solutions of a rodlike polymer (PBT) in polyphosphoric acid

A. F. Charlet and G. C. Berry*
Department of Chemistry, Carnegie Mellon University, Pittsburgh, PA 15213, USA
(Received 26 September 1988; accepted 26 November 1988)

Nematic solutions of the rodlike poly(1,4-phenylene-2,6-benzobisthiazole), PBT, in polyphosphoric acid, PPA, have been aligned in a shear flow to form a molecular composite. The tensile creep and recovery behaviour are studied to reveal a solidlike behaviour (no viscous flow) with a substantial Young's modulus E. X-ray diffraction studies show PBT to be aligned in the flow direction, and suggest that PPA oligomers may be oriented orthogonal to the PBT. The latter may reflect specific solvation of PBT by PPA. Values of E are compared with predictions from composite theory.

(Keywords: molecular composites; rodlike polymers; creep; nematic)

INTRODUCTION

In the processing of solutions of rodlike poly(1,4-phenylene-2,6-benzobisthiazole), PBT, to form fibres or films, the solutions are oriented in some flow field and then coagulated in a non-solvent[1]. Similar procedures have been studied to form molecular composites comprising mixtures of a rodlike polymer and a flexible chain polymer[2–5]. Here we report on properties of a gel phase formed before coagulation with solutions of PBT processed in polyphosphoric acid, PPA (weight fraction of P_2O_5 in the PPA equal to 83%). As shown in the following, this material has the attributes of a molecular composite, made rigid by the presence of a small fraction of a rigid, rodlike polymer.

EXPERIMENTAL

Solutions of PBT in PPA were formed into ribbons using an apparatus in which the solution is (slowly) forced onto the fact of a Mylar tape as the latter is pulled at constant velocity v through a (long) rectangular slot. The sample is subjected to shear flow in the gap between the tape and the stationary face of the slot. In the arrangement used, the width w and length L_s of the shearing zone in the slot were 0.6 cm and 6 cm, respectively, and the gap Δ between the tape and opposite stationary wall was 0.012 cm. The Mylar tape is moved with a capstan, which permits accurate control of v. The temperature of the slot is controlled by heat transfer with a circulating liquid. A nitrogen blanket is provided at the top of the shear zone to suppress premature coagulation of the solution. In this arrangement, the (nominal) shear rate κ is given by $\kappa = v/\Delta$, where v is the velocity of the Mylar tape, and the (nominal) total shear strain γ is equal to L_s/Δ, or 500 for the arrangement used in this study. In a steady-state flow, the cross-sectional area of the processed ribbon is expected to be $w\Delta/2$, or the weight W_L of a ribbon of length L is expected to be $\rho w \Delta L/2$, with ρ the solution density (approximately that of PPA); if W_L is expressed in denier, 1 denier being the weight in grams of 9000 m of ribbon, then W_L is expected to be about 7400 denier for the geometry used in this study.

Two nematic solutions were used, both prepared by polymerization of PBT monomers in PPA. Solutions were received through the courtesy of Dr J. F. Wolfe, SRI, International. The intrinsic viscosities of the polymers in these solutions were 2600 and 1400 $cm^3\ g^{-1}$ in solution in methane sulphonic acid for PBT-20 and PBT-32, respectively. The solutions of PBT-20 and PBT-32 had weight fraction PBT of 0.100 and 0.092, respectively. Rheological data on a solution of PBT-32 were obtained using methods and an apparatus described elsewhere[6,7]. Solutions were held under vacuum ($\approx 10^{-3}$ Torr; ≈ 100 Pa) at 120°C for three days before use. They were then placed into a glass centrifuge tube (50 ml) and centrifuged at about $10^4 g$ to consolidate the mass. This tube was placed in the pressure vessel at 160°C to supply the solution to the ribbon forming device (60–80 psi; 0.4–0.55 MPa).

Although in normal operation, the ribbons would be coagulated immediately on exiting the shearing head, in this study the ribbons were not coagulated, but collected and placed in a desiccator over P_2O_5 for storage until further use. The ribbon was not removed from the Mylar tape at this stage, and maintained the normal yellow–green colour of a PBT solution (as opposed to the red colour of the coagulated material). In most cases, two forms of the processed ribbon were used for creep studies: (1) the as-processed solution (removed from the Mylar tape); and (2) the same material after being coagulated, removed from the Mylar tape, and washed in water. In two cases, the processed solution was allowed to creep for $\approx 10^5$ s, under a stress of about 20 MPa, and then coagulated, washed and dried, while still under tension.

* To whom correspondence should be addressed

0032-3861/89/081462-05$03.00

A tensile creep apparatus described elsewhere[8] was used to determine the tensile creep compliance $D(t)$ of the as-processed PBT ribbons, still containing PPA (but removed from the Mylar tape), and the ribbon coagulated in water. In the latter case, the water was not removed from the coagulated ribbon. All measurements were at 30°C. With the creep apparatus, the ribbon is held between two clamps, one stationary and one movable, with a sample length L_T of about 4 cm. A weight W is applied to cause creep, or removed after some time to permit recovery. The applied tensile stress σ_T is calculated as $Wg\rho(9\times10^5)/W_L$ in CGS units, where W_L is the weight (g) of 9 km of the ribbon, i.e. W/W_L is the stress in g denier^{-1}. Values of W_L were determined by weighing a section of the sample of known length removed from the specimen between the two clamps. The strain $\varepsilon(t)$ is calculated as $\Delta l(t)/L_T$, where $\Delta l(t)$ is the displacement of the movable clamp at time t. The displacement was determined from the output of a linear variable differential transformer attached to the movable clamp. The creep compliance $D(t)$ is calculated as $\varepsilon(t)/\sigma_T$. The strain was also determined as a function of the time $\theta=t-t_c$ after cessation of creep of duration t_c. The recoverable strain $\varepsilon(\theta,t_c)$ is calculated as $\varepsilon(t_c)-\varepsilon(t)$ for $t>t_c$. In general, both $\varepsilon(t)$ and $\varepsilon(\theta,t_c)$ were determined over the range $10-6\times10^4$ s for a stress with $W=100$ g.

A flat plate camera was used to collect X-ray diffraction data on the processed ribbons. The sample was oriented with the long axis orthogonal to the meridian of the diffraction plane. Exposure times were typically 20 h.

RESULTS

Rheological data obtained[9] for PBT-32 at 40°C are shown in *Figure 1*, where η_κ is the steady-state viscosity at shear rate κ, and $\eta_d(\omega)$ is the linear dynamic viscosity at frequency ω. The properties of PBT-20 are similar, with η_κ larger. An unusual feature of the data in *Figure 1* is the non-equivalance of η_κ and $\eta_d(\omega)$ for $\kappa=\omega$. As with flexible chain polymers[10], such equivalence is usually observed with solutions of PBT in a solvent such as methane sulphonic acid[11]. For these solutions, the function $\eta_d(\omega)/\eta_s$ *versus* $\eta_s\omega$ is nearly independent of temperature, where η_s is the viscosity of the PPA solvent at temperature T (Reference 9). For the PPA used, η_s is proportional to $\exp[C_1/(T-C_2)]$ over the temperature range -10–80°C, with $C_1=856$ K and $C_2=200.5$ K, and η_s is 8.5 Pa s at 40°C.

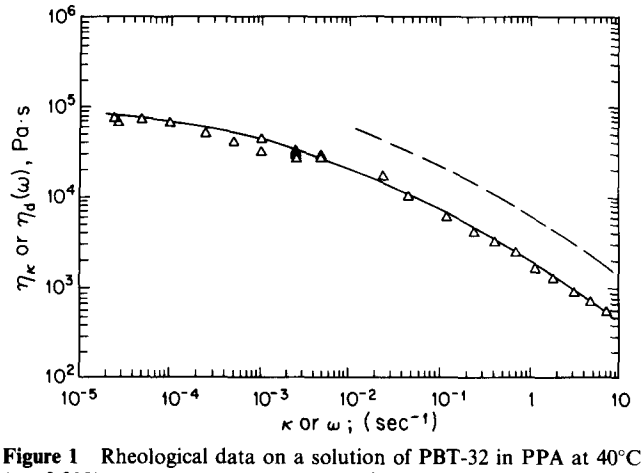

Figure 1 Rheological data on a solution of PBT-32 in PPA at 40°C ($w=0.092$). △, ——, η_κ *versus* κ; – – –, $\eta^*(\omega)$ *versus* ω

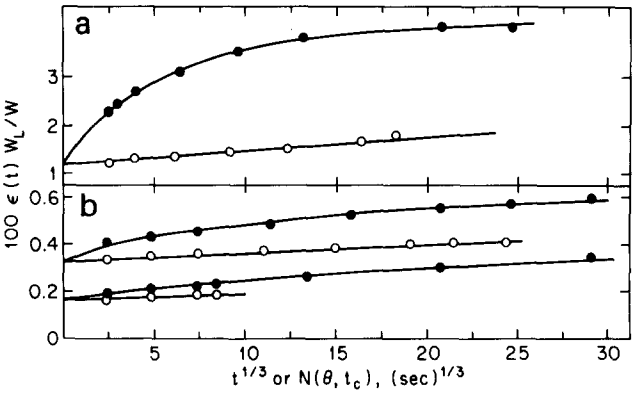

Figure 2 Tensile creep and recovery data on ribbons of PBT-20 in PPA at 30°C. ●, $100\varepsilon(t)W_L/W$ *versus* $t^{1/3}$; ○, $100\varepsilon(\theta,t_c)W_L/W$ *versus* $N(\theta,t_c)$; see equation (3). (a) Solution ($v/\Delta=5.3\,s^{-1}$). (b) Upper data set, wet coagulated ribbon ($v/\Delta=5.3\,s^{-1}$); and lower data set, dry sample prepared under tension ($v/\Delta=6.5\,s^{-1}$)

The experimental W_L for the processed solutions were in the range 700–1000 denier. Since this is much smaller than the expected value (7400 denier), it appears that solution was transported along only a small portion of the gap, i.e. the effective gap Δ_{eff} computed from the observed W_L as $\Delta_{eff}/\Delta=W_L/7400$ is found to be about 0.1Δ to 0.15Δ, with Δ_{eff} tending to decrease with increasing v. These results suggest that a thick, stagnant boundary layer is formed adjacent to the stationary surface. Values of W_L for the coagulated, wet ribbons are about 30% of the values for the solution, showing that the coagulated samples contain numerous voids, being about two-thirds by weight water.

Bilogarithmic plots of $\varepsilon(t)$ *versus* t or $\varepsilon(\theta,t_c)$ *versus* θ were nearly straight lines, with slope of 0.1 or less, and with $\varepsilon(t)$ larger than $\varepsilon(\theta,t_c)$ for $\theta=t$. In all cases, the recoverable creep had the form expected of Andrade creep. Thus, if $D(t)$ is given by

$$D(t)=D_{NR}(t)+D_R(t) \tag{1}$$

with $D_{NR}(t)$ and $D_R(t)$ the non-recoverable and recoverable creep, respectively, then for Andrade creep[12],

$$D_R(t)=D_0[1+(t/\tau_A)^{1/3}] \tag{2}$$

for $t<\tau_s$, and $D_R(t)=D_R(\tau_s)$ for $t\geqslant\tau_s$. Use of these relations and the assumption that $\varepsilon(\theta,t_c)$ may be computed according to formulae of linear viscoelasticity[12] gives[8]

$$\varepsilon(\theta,S)=\sigma_T D_0[1+N(\theta,t_c)/\tau_A^{1/3}] \tag{3a}$$

$$N(\theta,S)=t_c^{1/3}+\theta^{1/3}-(t_c+\theta)^{1/3} \tag{3b}$$

if $t_c<\tau_s$. As shown in *Figure 2*, the data on $\varepsilon(\theta,t_c)/\sigma_T$ *versus* $N(\theta,t_c)$ exhibit the expected linearity; similar behaviour was observed for all of the materials studied, resulting in the entries for $E_0=D_0^{-1}$ and τ_A listed in *Table 1*. In these entries ρ_0 is equal to the estimated ρ.

For linear viscoelastic behaviour, $D_{NR}(t)=t/\eta_E$, but as seen in *Figure 2*, the observed $\varepsilon(t)$ in creep do not increase linearly with t for large t and, in fact, $\varepsilon(t)$ increases more rapidly at small t than would be expected for the data on $\varepsilon(\theta,t_c)$. In all cases but one (see *Table 1*), the data obtained here can be fitted by a nonlinear form for $D_{NR}(t)$ given by

$$D_{NR}(t)=D_E\{1-\exp[-(t/\tau_E)^{1/3}]\} \tag{4}$$

where $D_E<D_0$ and $\tau_E<\tau_A$ for all of the samples studied.

Table 1 Parameters determined in creep and recovery

Polymer	Solution					Wet coagulated				Dry[b]			
	$v\Delta^{-1}$ (s^{-1})	$(\rho_0/\rho)E_0$[a] (GPa)	τ_A (ms)	E_0D_E	τ_E (s)	$(\rho_0/\rho)E_0$[a] (GPa)	τ_A (ms)	E_0D_E	τ_E (s)	$(\rho_0/\rho)E_0$[a] (GPa)	τ_A (ms)	E_0D_E	τ_E (s)
PBT-32 (92 g kg^{-1})	52	9.4	0.026	0.54	244	23.9	129	[c]	[c]	72.6	0.17	0.25	–
	83	11.7	0.024	0.57	91	–	–	–	–	–	–	–	–
PBT-20 (100 g kg^{-1})	5.3	14.0	0.16	1.91	91	30.1	0.76	0.48	216	–	–	–	–
	6.5	–	–	–	–	22.4	1.12	0.45	145	77.2	0.19	0.58	1000
	8.3	11.5	0.10	1.83	48	–	–	–	–	–	–	–	–
	9.5	20.3	0.34	0.97	215	25.2	11.09	0.52	420	–	–	–	–
	18.0	23.0	0.08	1.52	2300	28.5	3.69	1.12	145	–	–	–	–

[a] Calculated with ρ_0 equal to 2.3, 1.1 and 1.4 g cm^{-3} for the solutions, the wet coagulated, and the dry ribbons, respectively
[b] Coagulated, washed and dried under tension
[c] The creep could not be fitted with equation (4), but $\partial D_{NR}(t)/\partial t$ decreased with increasing t

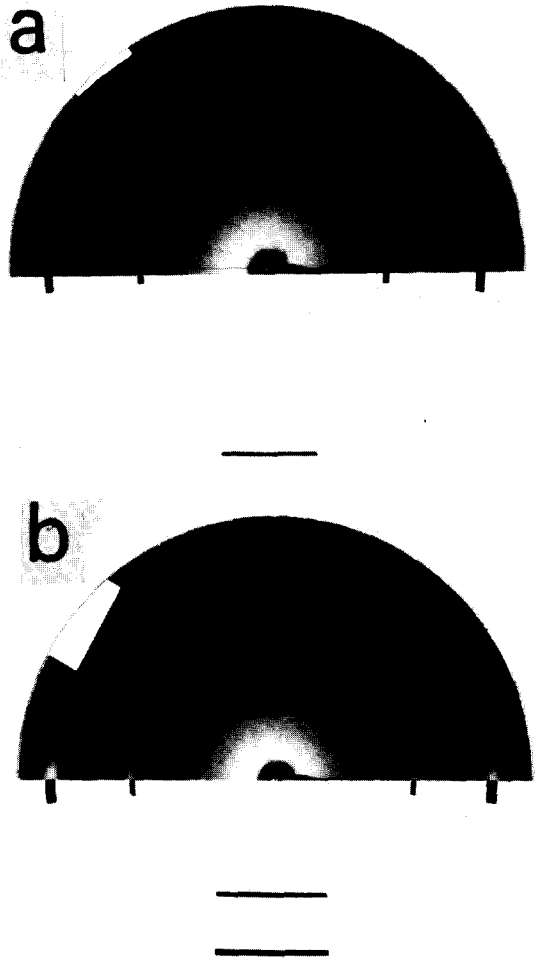

Figure 3 X-ray diffraction patterns for ribbons of PBT-20 in PPA. The ribbon longitudinal axis is along the meridian, with plane of the ribbon orthogonal to the incident beam. (a) Solution; (b) wet coagulated ribbon

Precedent for the use of a nonlinear form for $D_{NR}(t)$ to compute $\varepsilon(\theta, t_c)$ from $D(t)$ and the formulae of linear viscoelasticity exists for a number of cases[8]. For small t, equation (4) reduces to non-recoverable Andrade creep, also a nonlinear form, but with precedent in other materials[8]. Thus equation (4) may be considered to represent saturable, non-recoverable Andrade creep.

As seen in *Table 1*, similar behaviour was observed for the dried polymer and the solutions, though E_0 was larger and the creep smaller for the former. An appreciable increase in E_0 and decrease in creep was observed for the sample coagulated under tension.

The X-ray diffraction patterns obtained with an oriented solution and with a wet polymer recovered by coagulation are shown in *Figure 3*. Patterns similar to that for the solution were observed with all oriented solutions. The features shown in *Figure 3* are all absent in the scattering from an unoriented solution, and the arcs extend over a wider angle with samples less well oriented. The pattern for the solution exhibits meridional layer lines, at Bragg spacings of 0.62 and 0.41 nm, and two relatively sharp equatorial arcs at 0.52 and 0.345 nm (see *Figure 3*). For the dry polymer, the equatorial arc at 0.52 nm disappears and one at 0.59 nm appears, the layer line at 0.62 nm is absent, and that at 0.41 nm is less intense. These features are also seen in the X-ray pattern in *Figure 3* for the wet coagulated material.

DISCUSSION

The very low creep rate of the solutions is unexpected in view of the relatively high stress ($\approx$20 MPa) and the anticipated viscosity. The shear viscosity of the PPA solvent is about 18 Pa s at 30°C. Consequently, tensile creep measurements of the sort performed here would be impossible for the pure solvent. For a nematic fluid with a director alignment along the longitudinal axis, the elongational viscosity η_E and the shear viscosity η in slow flows are each functions of the order parameter of the equilibrium nematic fluid[13–16]:

$$\eta = \eta^{iso} H_{sh}(S) \tag{5}$$

$$\eta_E = 3\eta^{iso} H_E(S) = 3\eta H_E(S)/H_{sh}(S) \tag{6}$$

where η^{iso} depends on chain length and concentration, and $H_{sh}(S)$ and $H_E(S)$ each depend only on the (equilibrium) order parameter S, both being less than unity for S near unity. With one model[14–16],

$$\eta_E = 3\eta(1+S/2)^2/(1-S)(1+3S/2) \tag{7}$$

so that η_E may be much larger than η if S approaches unity. For sample PBT-32, η is of the order 10^6 Pa s at 27°C, so that except for very small t, $t/3\eta$ (the value of t/η_E for an isotropic fluid) far exceeds the observable $D(t)$; see *Figure 2*. For example, for the data in *Figure 2*, η_E would have to be of the order 10^{10} Pa s in order for the usual linear term t/η_E not to be evident in the measured $D(t)$. This is much larger than would be expected given the data on η.

The meridional lines in the X-ray diffraction from the solution are characteristic of PBT, and indicate that the molecular axis is aligned along the longitudinal axis of the ribbon[17–19]. The X-ray diffraction patterns from the solutions also exhibit a strongly oriented equatorial spacing at 0.52 nm. Whereas this spacing is absent in oriented PBT[17–19], it is characteristic of one form of ordered PPA, representing the repeat unit in a crystalline form of oligomers of the lithium salt of PPA[20]. In this structure, the PO_4 tetrahedra are linked with the 0.52 nm repeat corresponding to the span across two tetrahedra, with one edge of each tetrahedron on the PPA chain axis. The X-ray pattern suggests that the PPA oligomers giving the X-ray diffraction are oriented orthogonal to the axis of the oriented rodlike PBT chains. The equatorial 0.345 nm spacing is similar to a 0.362 nm spacing reported for oriented PBT[17–19], but may be from an entirely different origin, here originating in a distance of close approach of the PPA oligomer to the PBT chain.

The volume fraction ϕ of PBT estimated from the weight fraction w on the basis of volume additivity is given by

$$\phi = w(\rho_1/\rho_2)[1-(1-\rho_1/\rho_2)w]^{-1} \quad (8)$$

where ρ_1 and ρ_2 are the densities of PPA and PBT, respectively. Thus, for solutions of PBT in PPA, $\phi \approx 1.5w$ for $w \approx 0.1$. The cross-sectional area A_c of the volume occupied per chain is given by $M_L/\phi\rho_2 N_A$, with M_L equal to the mass per unit length, or $A_c = 1.6\ nm^2$ for $\phi = 0.16$, for PBT. In a well aligned sample with all chains parallel, A_c may be expressed as gd_1d_2, where g is a geometric factor of order unity, and d_1 and d_2 represent mutually orthogonal mean chain separations perpendicular to the chain axis. In this case, A_c is large enough that the chains may be well separated on average, unless the chain is construed to include a coordinated solvent. A minimum value of 0.35 nm for d_2, corresponding to stacking of the PBT planes, would give a maximum d_1 of 4.5 nm. It is likely that d_1 is smaller and d_2 larger than these estimates, and that the coordinated PPA oligomers on adjacent chains are close enough to interact with each other. Longer oligomers may coordinate with adjacent chains, forming a crosslink. This postulate is enforced by the observation that $\eta^d(\omega) > \eta_\kappa$ for $\kappa = \omega$. The smaller η_κ may result from the (partial) destruction of structure in steady flow, whereas that structure remains intact under low amplitude sinusoidal deformation. Either substantial interaction among the PPA on the solvated chains, or crosslinking involving the PPA, could be responsible for the low creep and the absence of flow (i.e. apparently infinite η_E) found for the processed solutions. Other forms of PBT–PPA solvation have been examined by X-ray studies on solutions containing various amounts of water[21].

The preceding suggests that the solutions be considered a molecular composite, with rodlike PBT aligned in a low modulus solid. The $E_0 = D(0)^{-1}$ exhibit a tendency to increase with increasing v, as would be expected if the alignment increased with increasing v. Further, as seen in *Table 1*, E_0 is enhanced by coagulation and drying under tension. This may correspond to enhanced alignment during the small creep that does occur. In the context, E_0 might be estimated from the moduli of the two components using relations developed for a composite comprising rods dispersed in a solid matrix. According to the analysis of Halpin and Tsai[22] for the modulus E_c of a composite comprising an isotropic matrix (modulus E_m) with completely aligned dispersed rods (modulus E_R, length L, and diameter d)

$$E_c = E_m(1+\xi\eta\phi)/(1-\eta\phi) \quad (9a)$$

$$\eta = (R-1)/(R+\xi) \quad (9b)$$

where $\xi = 2L/d$ and $R = E_R/E_m$. In the limit of infinite ξ, equation (9) reduces to

$$E_c = (1-\phi)E_m + \phi E_R \quad (10)$$

corresponding to the often cited 'rule-of-mixtures' approximation for E_c.

Theoretical estimates give a modulus $E_{PBT} \approx 600$ GPa for the PBT chain[23]. If this value is used as E_R in equation (10), then with neglect of $E_m \ll E_{PBT}$, $E_c \approx \phi E_{PBT}$ is calculated to be 96 GPa, which is larger than the maximum modulus $E_0 = 23$ GPa observed for a processed solution. Several factors may contribute to this discrepancy including: (1) the use of equations (9) and (10) for a molecularly dispersed system, whereas they were developed for a dispersion of macroscopic particles in a continuum; (2) the effects of a finite L/d ratio for the dispersed rodlike chains; (3) the effects of imperfect alignment of the rodlike chains; and (4) an erroneous estimate of E_{PBT}. Since the modulus of well aligned PBT fibres approaches $0.4E_{PBT}$ (Reference 23), the estimate for E_{PBT} seems to be acceptable at present. The calculated value is also in reasonable accord with measurements of $E_0 \approx 0.7E_{PBT}$ for fibres based on the change in the layer line spacing under a tensile load[23]. The effects of finite L/d given by equation (9) take the form

$$E_c \approx XE_R\phi/(1+X) \quad (11)$$

for small ϕ, $\xi \gg 1$ and $E_R \gg E_m$, where $X = \xi E_m/E_R$. In this case, E_c may be substantially reduced from the value given by equation (10). If E_m is taken to be the value of the tensile modulus $E(t)$ at 0.1 s for PPA, then $E_m \approx 250$ Pa, or $E_m/E_{PBT} \approx 4 \times 10^{-10}$. Thus, for any reasonable ξ, equation (11) reduces to $E_c \approx \xi E_m \phi$. This is much smaller than the observed E_0 if $\xi \approx 10^2$, which is in the expected range.

Alternatively, the low value of E_c could result from distribution of L among the chains, or imperfect alignment of the PBT rods along the longitudinal ribbon axis. Such effects have been estimated by calculations based on the laminate analogy, in which the composite behaviour is modelled as that for a material comprising layers, each layer with well aligned monodisperse rods, the number of each such layer being proportional to the fraction of such alignments in the composite[22,24,25]. Calculations of misalignment effect on E_c for a certain distribution of the alignment angle α of the rods relative to the ribbon axis[26] give results that may be expressed in the form of equation (11) (for the stipulated $\phi < 1$, $\xi \gg 1$ and $E_R \gg E_m$), with $\xi E_m/E_R$ in the denominator replaced by a function $P(\xi E_m/E_R, \langle\cos^2\alpha\rangle, \phi)$ dependent on the distribution of α, as well as on $\xi E_m/E_R$ and ϕ. As expected, misalignment reduces E_c below the value given by equation (11). Consequently, such effects would not seem to be the cause of the large E_0 observed here.

The observed $E_0 = 23$ GPa would require $\xi E_m/E_R \approx 0.24$, using equation (9). Use of the preceding estimate of E_m/E_{PBT} for E_m/E_R would correspond to an unreasonably large L/d based on molecular dimensions. On the other hand, use of $\xi E_m/E_R \approx 0.24$ with $L/d = 100$ would require

$E_R/E_m \approx 800$ to reproduce the experimental data. This could imply that E_m for PPA in the composite is much greater than $E(t)$ for bulk PPA at $t=0.1$ s, which could occur if the PPA is ordered in the solution, as suggested by the X-ray data. Thus, the high values of E_0 appear to result from the combined effects of reinforcement from the stiff PBT chains and enhanced E_m for the matrix forming the molecular composite.

ACKNOWLEDGEMENT

This study was supported in part by the Polymers Branch, Nonmetallic Materials Division, Wright–Patterson Air Force Base. It represents partial fulfilment of the requirements for the MS (Chemistry) degree for A.F.C.

REFERENCES

1 Allen, S. R., Filippov, A. G., Farris, R. J., Thomas, E. L., Wong, C.-P., Berry, G. C. and Chenevey, E. C. *Macromolecules* 1981, **14**, 1135
2 Helminiak, T. E., Benner, C. L. and Arnold, F. E. *Polym. Prepr. Am. Chem. Soc.* 1975, **16** (2), 659
3 Takayanagi, M., Ogata, T., Morikawa, M. and Kai, T. *J. Macromol. Sci. Phys.* (*B*) 1980, **17**, 591
4 Hwang, W.-F., Wiff, D. R., Benner, C. L. and Helminiak, T. E. *J. Macromol. Sci. Phys.* (*B*) 1983, **22**, 231
5 Takayanagi, M. *Pure Appl. Chem.* 1983, **55**, 819
6 Chu, S. G., Venkatraman, S., Berry, G. C. and Einaga, Y. *Macromolecules* 1981, **14**, 939
7 Venkatraman, S., Berry, G. C. and Einaga, Y. *J. Polym. Sci., Polym. Phys. Edn.* 1985, **23**, 1275
8 Berry, G. C. *J. Polym. Sci. Polym. Phys. Edn.* 1976, **14**, 451
9 Tsai, H. H. Phase Equilibrium and Rheological Studies of Rodlike, Articulated Polymers and Their Mixture, Ph.D. Thesis, Carnegie-Mellon University, USA, 1983
10 Cox, W. P. and Merz, B. H. *J. Polym. Sci.* 1958, **28**, 619
11 Berry, G. C. Unpublished results
12 Berry, G. C. and Plazek, D. J. in 'Glass: Science and Technology', Vol. 3 (Eds. D. R. Uhlmann and N. J. Kreidl), Academic Press, New York, 1986, Ch. 6
13 Doi, M. and Edwards, S. F. 'The Theory of Polymer Dynamics', Clarendon Press, Oxford, 1986
14 Marrucci, G. *Mol. Cryst. Liq. Cryst. Lett.* 1982, **72**, 153
15 Kuzuu, N. and Doi, M. *J. Phys. Soc. Japan* 1983, **52**, 3489
16 Berry, G. C. *Mol. Cryst. Liq. Cryst.* in press
17 Adams, W. W., Azaroff, L. V. and Kulsheshtha, A. K. *Z. Krist.* 1979, **115**, 321
18 Roche, E. J., Takahashi, T. and Thomas, E. L. *Am. Chem. Soc. Symp.* 1980, **141**, 303
19 Odell, J. A., Keller, A., Atkins, E. D. T. and Miles, M. J. *J. Mat. Sci.* 1981, **16**, 3309
20 Thilo, E. *Adv. Inorg. Chem. Radiochem.* 1962, **4**, 1
21 Saruyama, Y., Cohen, Y. and Thomas, E. L. In preparation
22 Ashton, J. E., Halpin, J. C. and Petit, P. H. 'Primer on Composite Materials: Analysis', Technomic Publ. Co., Stanford, CN, USA, 1969, p. 77
23 Adams, W. W. and Wierschke, S. G. In preparation
24 Halpin, J. C. and Pagano, N. J. *J. Comp. Materials* 1969, **3**, 720
25 Halpin, J. C., Jerine, K. and Whitney, J. M. *J. Comp. Materials* 1971, **5**, 36
26 Donaldson, S. L. Personal communication